

The Inverse Relationship between Metal-Enhanced Fluorescence and Fluorophore-Induced Plasmonic Current

Joshua Moskowitz and Chris D. Geddes*



Cite This: *J. Phys. Chem. Lett.* 2020, 11, 8145–8151



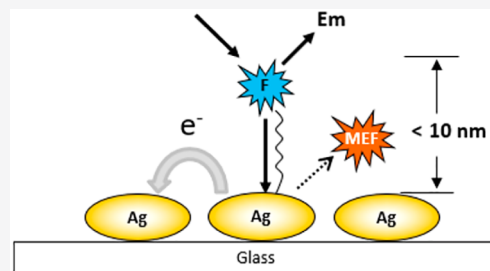
Read Online

ACCESS |

Metrics & More

Article Recommendations

ABSTRACT: In this work we investigate the relationship between metal-enhanced fluorescence (MEF) and fluorophore-induced plasmonic current (PC). This is accomplished through measurements of both radiative emission (MEF) and direct electrical current generation between discrete metal nanoparticles upon fluorophore excitation (PC). We have conducted these measurements on silver and gold nanoparticle island films, over a range of nanoparticle sizes and spacing in the films. We have observed an inverse relationship in the magnitude of MEF with PC, where larger and more closely spaced metal nanoparticles are found to result in increased PC and subsequently a decreased MEF. We attribute this effect to the relatively high capacitance and low charging energy of large and closely spaced particles, providing an outlet for plasmon relaxation in the form of electron flow and electrical current generation. These results are significant as they open potential for controlling for and the optimization of both MEF and PC.



Recent advances in the understanding of metal-enhanced fluorescence (MEF) and fluorophore-induced plasmonic current (PC) have led to the development of both optical and photovoltaic devices, respectively. These devices operate either through “plasmon to light” optical far-field detection such as in MEF and surface plasmon resonance (SPR),^{1–12} or by “plasmon to current” direct electrical current generation resulting from the dephasing of plasmon resonance.^{13–17} This direct electrical current generation may be accomplished using plasmon resonance in conjunction with a semiconducting material,^{13,14} or through electron transport between closely spaced metal nanoparticles such as in PC.^{15,16} In both MEF and PC, a fluorophore may be used for nonradiative energy transfer to a metal nanoparticle, resulting in plasmon excitation. The excited plasmon may then relax through various routes, including radiative emission, heat loss to the surroundings, and electron transport.^{15,16} While extensive literature is available regarding both optical and photovoltaic techniques separately, little has been published regarding the relationship between these two phenomena.

MEF has been studied extensively by various groups, with much information available in the literature.^{1–10} In MEF, a metal nanoparticle may use its relatively large size to act as a nanoantenna for light capture, effectively increasing the absorption cross section of a proximal fluorophore.^{1,18} The fluorophore may then nonradiatively transfer energy to the metal nanoparticle, with subsequent emission from the metal itself at a frequency mostly characteristic of the fluorophore.^{1,7,8} This emission has been found to be more intense and with a decreased fluorescence lifetime as compared to the free-space fluorophore without the metal.^{1,5,6} This emission is then

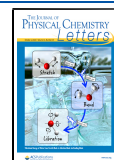
typically detected by a far-field photodetector, providing information regarding the fluorophore and allowing for the construction of various detection assays (Figure 1a).

PC is generated when a fluorophore nonradiatively transfers energy to a proximal metal nanoparticle island film, resulting in a measurable current change through the film.^{15–17} This is possible because of close spacing between discrete metal nanoparticles in the film, allowing for electron transport between the particles, also known in the literature as electron “hopping” (Figure 1b,c).^{19–23} Previous work from our laboratory has also shown the electrical current change upon fluorophore excitation to be dependent on the magnitude of the fluorophore extinction coefficient,¹⁵ providing information regarding the fluorophore and opening the possibility for various detection assays. This dependence of the current on fluorophore extinction coefficient is explained by the capability of a higher extinction fluorophore to bring more energy into proximity of the metal nanoparticle, allowing for increased energy transfer to the metal, and a subsequent increase in current generation through the film upon fluorophore excitation. Electron transport between discrete metal particles in the film is dependent on the capacitance and charging energy of metal nanoparticles in the film and has been

Received: June 26, 2020

Accepted: September 4, 2020

Published: September 4, 2020



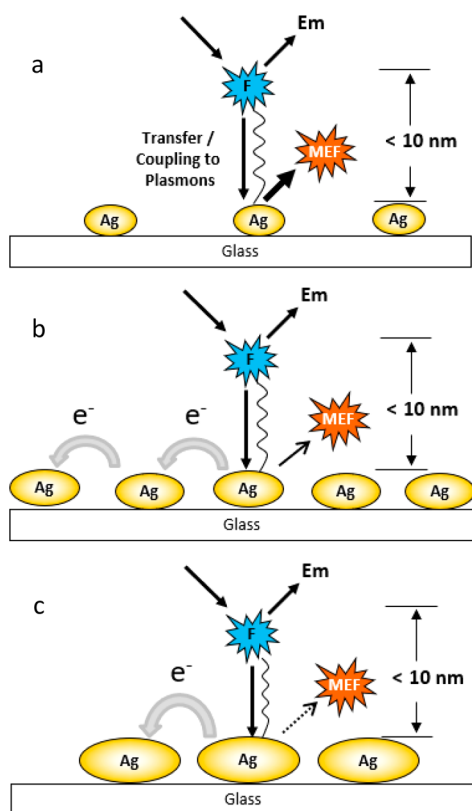


Figure 1. Cartoon depicting both metal-enhanced fluorescence (MEF) and fluorophore-induced plasmonic current generation (PC). (a) For isolated noncontinuous nanoparticulate surfaces, the silver nanoparticles are spaced far enough apart to facilitate MEF but also perturb plasmonic current flow. (b) As the nanoparticles increase in size and their interparticle spacing decreases, both PC and MEF can be observed. (c) As the particles grow larger and their interparticle spacing significantly decreases, PC becomes more favorable over MEF.

described in detail in recent work from our laboratory.^{15,16} Larger and more closely spaced discrete nanoparticles have been found to provide for increased particle capacitance and decreased particle charging energy, leading to increased fluorophore-induced current generation.¹⁶ This is significant, as it represents a method of increasing plasmonic current, simply by making metal particles in the film larger and more closely spaced (Figure 1c). In addition, nanoparticles used in

this work are relatively large (~ 50 nm) and do not couple strongly with the far-field laser light because of a wavevector mismatch between the far-field radiation and the metal particle. However, a proximal fluorophore may still couple with and excite plasmons locally in the near-electric field of the metal particle.¹⁵

In this work we investigate the relationship between MEF and PC through measurements of both far-field radiative emission (MEF) and direct electrical current generation between discrete metal nanoparticles upon fluorophore excitation (PC). This is carried out utilizing metal nanoparticles of various size and spacing in order to alter the electronic properties of the metal nanoparticle island film and better understand the relationship between MEF and PC. Understanding this relationship is critical in the optimization of nanoparticle arrays for assay development in both optical and direct electrical “plasmon to current” techniques.

Silver and gold nanoparticle island films were prepared via thermal vapor deposition as described in previous work from our laboratory.^{15,16} Briefly, Silane-prep slides (Sigma-Aldrich) were cleaned with methanol, dried under N_2 , and used as a substrate for thermal vapor deposition. The deposition rate was held constant at 0.1 \AA/s with a range of vapor deposition times. Electrical current through the system was monitored with a Keithley 6487 picoammeter/voltage source, in an open-circuit configuration. Electrode materials were selected to match the metal nanoparticle film (for example silver-on-silver). The electrodes were positioned to make simultaneous contact with the metal nanoparticle film and the liquid solvent.

PC measurements were undertaken in a manner similar to previous work from our laboratory.^{15,16} Briefly, fluorophore solutions were prepared in deionized water and pipetted onto the metal nanoparticle island films. Fluorophores were then excited with either a 473 or 594 nm *p*-polarized continuous wave laser directed at the film surface. Laser power was controlled with an absorbing neutral density filter (Edmund Optics) and held constant at a power of 10 mW. Change in electrical current through the system was reported as the absolute value of current change, ΔI , upon application of the fluorophore excitation source. Fluorescence emission measurements were obtained through a fiber optic collection cable positioned above the film surface, which carried the radiative emission to a connected spectrophotometer with external computer display. An experimental schematic is depicted in Figure 2.

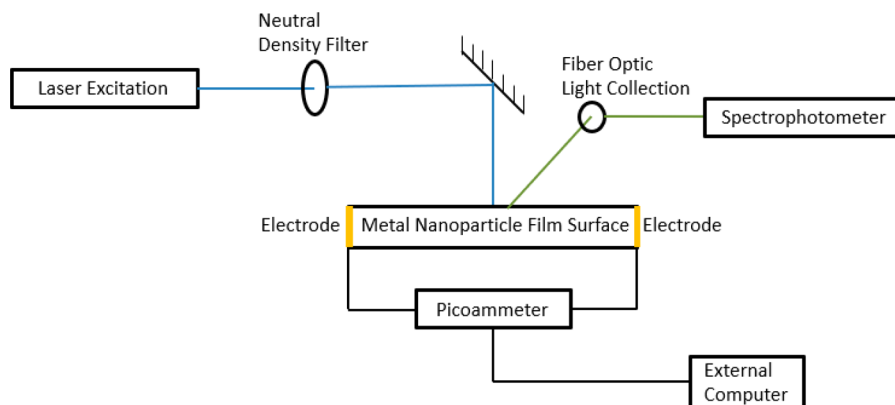


Figure 2. Schematic depicting the experimental MEF-PE optical train.

UV–vis absorbance spectra of typical silver and gold nanoparticle island films over a range of film thermal vapor deposition times have been reported in previous work from our laboratory.¹⁶ Increased thermal vapor deposition led to red-shifted and broadened absorbance spectra, indicating the growing of the average particle size in the film. As these particle sizes in the film increase, the spacing between the particles decreases. In other words, the particles grow into each other, starting to form connections toward the eventual formation of a continuous metal film.^{15,16} This is supported by representative scanning electron microscopy images of the films, which are also reported in previous work from our laboratory.^{15,16} Films may be characterized as either electrically non-, semi-, or fully continuous metal films. Here, dry noncontinuous films display zero measurable current in the absence of an applied bias. Dry semicontinuous metal nanoparticle films display a small current in the absence of an applied bias due to some metal pathways forming across the film. In contrast, fully continuous films display a relatively high current and low resistance of $\sim 1 \Omega$ in the absence of an applied bias (Figure 3).

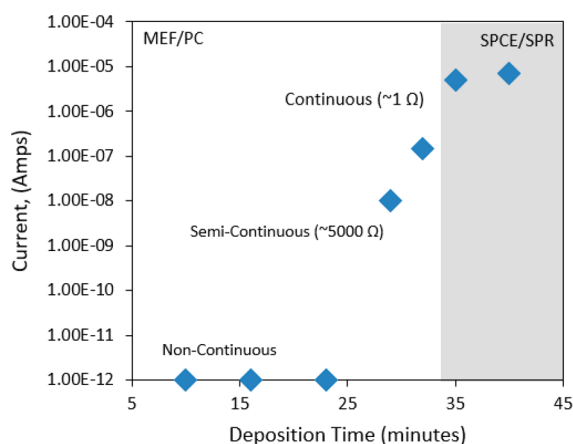


Figure 3. Electrical current through dry gold films produced via thermal vapor deposition at various deposition times. The deposition was performed at a constant pressure and constant deposition rate of 9×10^{-6} Torr and 0.1 \AA/s , respectively. At long deposition times, the films are relatively thicker and ideally suited for SPCE (surface plasmon coupled emission) or SPR (surface plasmon resonance) experiments. Thinner films with resistances below $\sim 5000 \Omega$ are ideally suited for metal-enhanced fluorescence (MEF) and plasmonic current (PC) measurements.

PC in our films is found to be largest in noncontinuous films (Figure 4). This is explained by the fact that in semi- and fully continuous metal films, the background current due to current flow through the metal is relatively high, hindering the observation of a large current change with excitation of the fluorophore.

Silver and gold films used for investigation of the relationship between MEF and PC in this work were electrically noncontinuous and brought as close as possible to semicontinuous films, without forming pathways across the film for electron transport. Increasing particle size and decreasing particle spacing in the film increase the metal particle capacitance according to the concentric sphere model.^{15,16,22,23}

$$C = 4\pi\epsilon_0\epsilon r_0(r_0 + s)/s \quad (1)$$

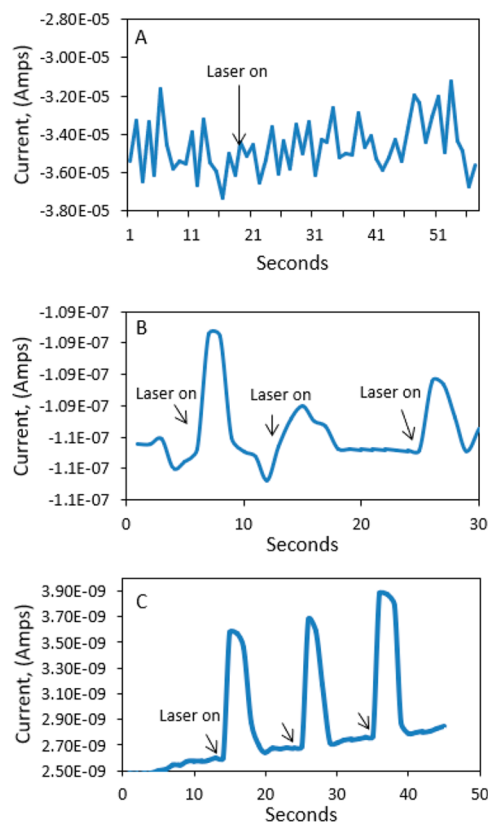


Figure 4. Electrical current generation from the excitation of $10 \mu\text{M}$ Fluorescein di-sodium salt solutions on continuous (A), semi-continuous (B), and noncontinuous (C) silver-island films. Arrows indicate when the excitation light was applied.

where ϵ_0 is the vacuum permittivity, ϵ the static relative permittivity of the medium surrounding the particle, r_0 the particle radius, and s the distance between two neighboring particles.^{22,24–27}

The particle capacitance is then related to the charging energy required for the metal nanoparticle to gain an electron by

$$E_C = \frac{e^2}{2C} \quad (2)$$

where E_C is charging energy, e the elementary electric charge, and C capacitance of the particle.^{20,22} A detailed description of metal nanoparticle capacitance and charging energy in our films is provided in previous work from our laboratory.¹⁵ Essentially, electron transport is favored in larger and more closely spaced particles.

Figure 5 shows measurements of both MEF and PC with silver nanoparticle island films produced over a range of thermal vapor deposition times in order to alter particle size and spacing in the films.¹⁶ Fluorescein was chosen as the fluorophore in this experiment because of the large overlap between its emission and the silver nanoparticle film absorbance, providing for optimal energy transfer.^{1,2,7} Increasing particle size and decreasing spacing between the particles was found to result in an increased current change upon fluorophore excitation, thought to be due to the increased tendency for electron transport between the closely spaced discrete nanoparticles. In contrast, MEF was found to be greatest in the relatively small and far spaced nanoparticle

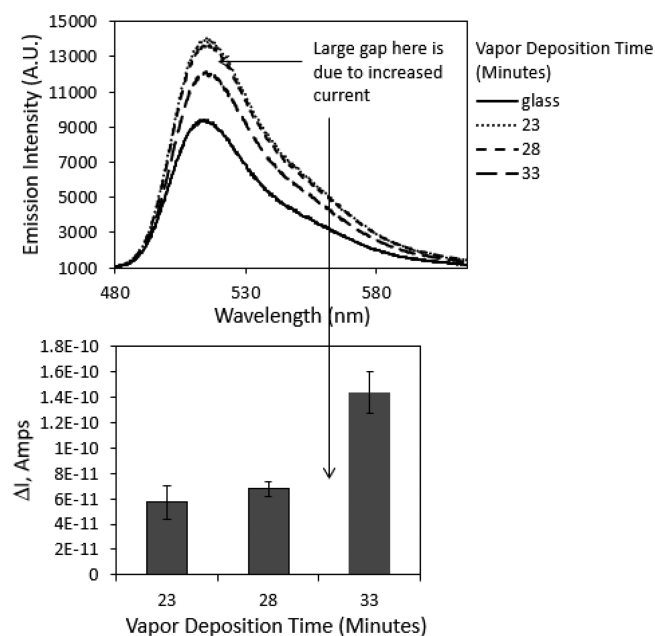


Figure 5. (Top) MEF from 10 μM fluorescein *di*-sodium salt solutions from various silver films, vapor deposited at different times, and (bottom) corresponding fluorophore-induced plasmonic current, ΔI . Each point is an average of three laser exposures and subsequent current measurements, with error bars calculated as the standard deviation of these three measurements. The deposition was performed at a constant pressure and constant deposition rate of 9×10^{-6} Torr and 0.1 $\text{\AA}/\text{s}$, respectively.

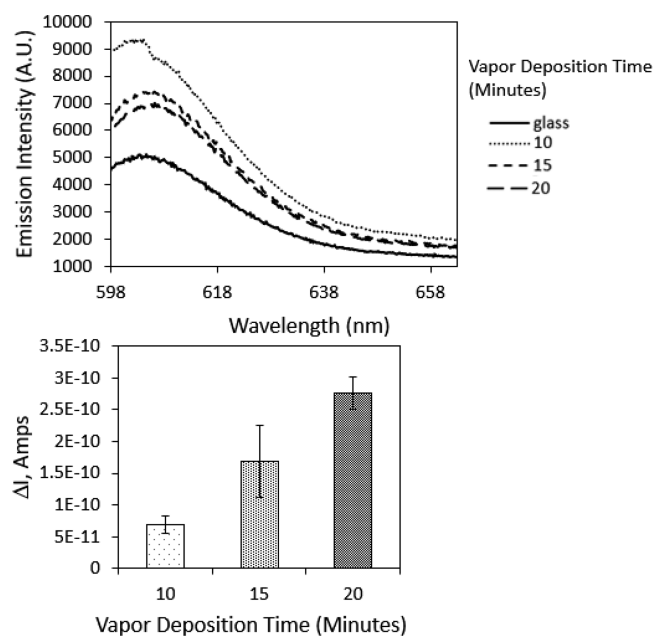


Figure 6. (Top) MEF from 10 μM sulforhodamine 101 aqueous solutions on various gold films, vapor deposited at different times, and (bottom) corresponding fluorophore-induced plasmonic current, ΔI . Each point is an average of three laser exposures and subsequent current measurements, with error bars calculated as the standard deviation of these three measurements. The deposition was performed at a constant pressure and constant deposition rate of 9×10^{-6} Torr and 0.1 $\text{\AA}/\text{s}$, respectively.

substrates, demonstrating an inverse relationship with PC, as expected. This observation is attributed to the very close spacing of nanoparticles in the film providing a mechanism for plasmon dephasing in the form of electron transport, essentially turning off MEF. In other words, upon plasmon excitation, relatively small and isolated nanoparticles are more likely to relax via radiative emission compared to very closely spaced nanoparticles, which may relax via electron transport.

In addition to silver, a similar experiment was carried out with gold nanoparticle island films produced over a range of thermal vapor deposition times, subsequently altering the particle size and spacing within the films. Representative scanning electron microscopy images of very similar films in previous work from our laboratory show the gold particles to be less spherical compared to the silver particles, with more complex geometrical shapes.¹⁵ Investigation of the relationship between MEF and PC on gold island films was carried out using sulforhodamine 101 as the fluorophore, which emits at 594 nm, providing for a large overlap with the gold film absorbance. A similar inverse relationship between MEF and PC was observed in these gold films as with the silver films, with increased PC and decreased MEF observed in films composed of large and very closely spaced metal nanoparticles (Figure 6).

We have additionally investigated fluorophore photostability on various silver nanoparticle island films in order to better understand the relationship between MEF and PC. The effect of proximal metal nanoparticles on fluorophore photostability has been previously studied in the literature, and the observation of an increased fluorophore photostability in the presence of metal nanoparticle films has been reported many times.^{28,29} This enhanced photostability has been attributed to

the decreased fluorescence lifetime of the metal–fluorophore coupled system.^{28,29} This is because if the fluorophore spends less time in the excited state when coupled to a metal nanoparticle, then it is less susceptible to excited-state photodestructive processes such as photooxidation,²⁹ which would ultimately decrease photostability. In other words, energy transfer from the fluorophore to metal and subsequent fast emission from the metal is thought to protect the fluorophore from photobleaching,^{28,29} resulting in the observed photostability increase in the presence of metal nanoparticles. These photostability investigations do not provide an assessment of the fluorophore radiative lifetime on the various nanoparticle films, and the effect of these various films (high MEF and high PC) on the radiative lifetime is currently unknown.

We subsequently measured fluorescence intensity decay curves (i.e., photon flux vs time) for fluorescein on various silver island films, providing photostability information regarding both high MEF and inversely high PC supporting films. Decay time constants were calculated as the time required for the signal to decay to $1/e$ of the initial intensity. Relatively small and far spaced nanoparticles (high MEF) were found to provide for increased photostability compared to a glass control, supporting previous MEF photostability studies in the literature.^{28,29} However, very large and closely spaced nanoparticles (high PC) were found to result in a *relatively decreased* fluorophore photostability. An overall trend of decreasing fluorophore photostability with increasing nanoparticle size was observed (Figure 7). This observation may be explained by the MEF “turn off” effect reducing the fluorescence intensity through time, with an increasing number of fluorophores losing energy to the metal as a function of time

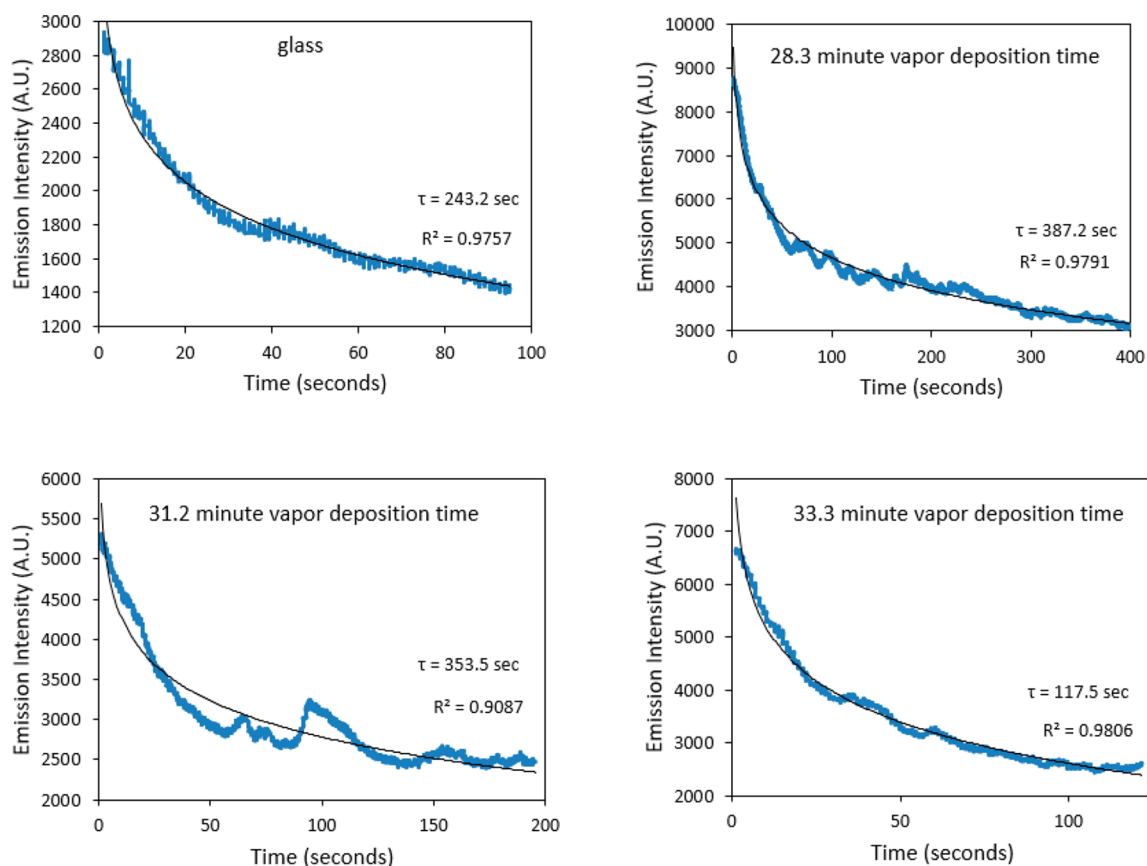


Figure 7. Fluorescence emission intensity versus time (photostability) from 10 μM fluorescein solutions on silver island films made with various thermal vapor deposition times, with 10 mW 473 nm excitation. Decay time constants (τ) were calculated as the time required for the fluorescence emission to decay to $1/e$ of the initial intensity.

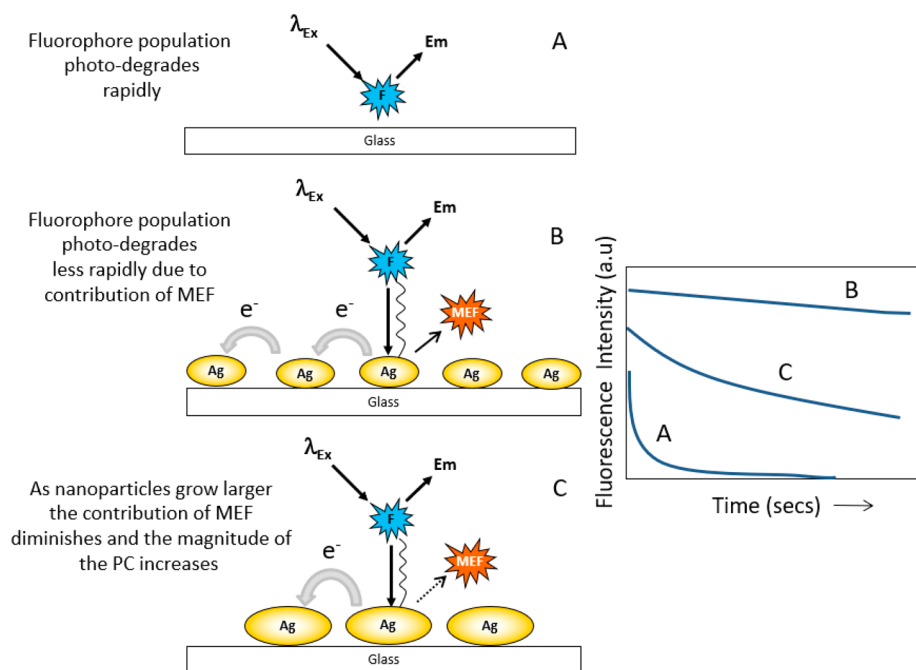


Figure 8. Cartoon depicting the photostability of fluorophores on both glass (A) and increasing size (B \rightarrow C) of metallic nanoparticles. (A) Photostability (fluorescence intensity vs time) of a solution of fluorophore from a glass substrate; (B) photostability of a solution of fluorophore from silver nanoparticle coated glass, and (C) photostability from larger sized nanoparticle deposited glass. As the nanoparticles grow in size, the magnitude of induced plasmonic current (PC) increases, while the contribution of MEF decreases. MEF contributes to the system photostability, whereas fluorophores which generate PC do not, as these become nonfluorescent (MEF, metal-enhanced fluorescence).

in the relatively large and closely spaced nanoparticles (Figure 8). This is supported by studies in the literature involving the voltage gating (or turning off) of MEF, in which emission intensity is found to decrease exponentially over time following an applied voltage.^{30,31} This result is significant as it describes a difference in the photostability of a fluorophore–metal nanoparticle coupled system with nanoparticle size and spacing optimized for either MEF or fluorophore-induced current generation.

In conclusion, we have observed an inverse relationship between metal-enhanced fluorescence (MEF) and fluorophore-induced plasmonic current (PC). This was accomplished through measurements of both radiative fluorescence emission and electrical current with fluorophore excitation on a metal nanoparticle island film. It was found that increasing nanoparticle size and decreasing spacing between adjacent particles in the film provided for increased current generation and decreased radiative emission. This is explained by an increase in particle capacitance in the large particles, favoring plasmon relaxation via current generation as opposed to plasmon relaxation via radiative emission in the relatively small nanoparticles. This finding is significant as it allows for controlling between metal-enhanced radiative emission and fluorophore-induced current simply by altering the size and spacing of metal nanoparticles in the film. In addition, we have obtained fluorescence intensity decay curves on various silver island films, providing information regarding fluorophore photostability on films optimized for either MEF or plasmonic current. Here it was observed that relatively large and closely spaced particles resulted in a decrease in fluorophore photostability, which we attribute to an increase in fluorophore-to-metal energy transfer through time in these large and closely spaced metal nanoparticles.

AUTHOR INFORMATION

Corresponding Author

Chris D. Geddes – Institute of Fluorescence and Department of Chemistry and Biochemistry, University of Maryland Baltimore County, Baltimore, Maryland 21202, United States;
Email: Geddes@umbc.edu

Author

Joshua Moskowitz – Institute of Fluorescence and Department of Chemistry and Biochemistry, University of Maryland Baltimore County, Baltimore, Maryland 21202, United States;
orcid.org/0000-0002-4768-9082

Complete contact information is available at:
<https://pubs.acs.org/10.1021/acs.jpcllett.0c01973>

Notes

The authors declare no competing financial interest.

ACKNOWLEDGMENTS

The authors thank the Institute of Fluorescence as well as the Department of Chemistry and Biochemistry at the University of Maryland Baltimore County (UMBC) for financial support.

REFERENCES

- (1) Lakowicz, J. R. *Principles of Fluorescence Spectroscopy*, 3rd ed.; Springer: New York, 2006; pp 841–867.
- (2) Geddes, C. D.; Lakowicz, J. R. Metal-Enhanced Fluorescence. *J. Fluoresc.* **2002**, *12*, 121–129.

- (3) Eustis, S.; El-Sayed, M. Aspect Ratio Dependence of the Enhanced Fluorescence Intensity of Gold Nanorods: Experimental And Simulation Study. *J. Phys. Chem. B* **2005**, *109* (34), 16350–16356.

- (4) Pelton, M.; Bryant, G. W. *Introduction to metal-nanoparticle plasmonics*; Wiley: Hoboken, NJ, 2013.

- (5) Li, J.; Krasavin, A. V.; Webster, L.; Segovia, P.; Zayats, A. V.; Richards, D. Spectral Variation of Fluorescence Lifetime Near Single Metal Nanoparticles. *Sci. Rep.* **2016**, *6*, 21349.

- (6) Weitz, D. A.; Garoff, S.; Hanson, C. D.; Gramila, T. J.; Gersten, J. I. Fluorescent Lifetimes Of Molecules on Silver-Island Films. *Opt. Lett.* **1982**, *7* (2), 89–91.

- (7) Geddes, C. D. *Metal-Enhanced Fluorescence*; Wiley: Hoboken, NJ, 2010; pp 1–20.

- (8) Zhang, Y.; Dragan, A.; Geddes, C. D. Wavelength Dependence of Metal-Enhanced Fluorescence. *J. Phys. Chem. C* **2009**, *113* (28), 12095–12100.

- (9) Pribik, R.; Dragan, A. I.; Zhang, Y.; Gaydos, C.; Geddes, C. D. Metal-enhanced fluorescence (MEF): physical characterization of Silver-island films and exploring sample geometries. *Chem. Phys. Lett.* **2009**, *478* (1), 70–74.

- (10) Zhang, Y.; Aslan, K.; Previte, M. J. R.; Geddes, C. D. Metal-Enhanced E- Type Fluorescence. *Appl. Phys. Lett.* **2008**, *92* (1), 013905.

- (11) Jeanmaire, D. L.; Van Duyne, R. P. Surface Raman Spectroelectrochemistry. Part I. Heterocyclic, Aromatic, And Aliphatic Amines Adsorbed On The Anodized Silver Electrode. *J. Electroanal. Chem. Interfacial Electrochem.* **1977**, *84*, 1–20.

- (12) Le Ru, E. C.; Blackie, E.; Meyer, M.; Etchegoin, P. G. Surface Enhanced Raman Scattering Enhancement Factors: A Comprehensive Study. *J. Phys. Chem. C* **2007**, *111* (37), 13794–13803.

- (13) Tang, L.; Kocabas, S. E.; Latif, S.; Okyay, A. K.; Ly-Gagnon, D. S.; Saraswat, K. C.; Miller, D. A. Nanometre-Scale Germanium Photodetector Enhanced By A Near-Infrared Dipole Antenna. *Nat. Photonics* **2008**, *2* (4), 226–229.

- (14) Falk, A. L.; Koppens, F. L.; Yu, C. L.; Kang, K.; de Leon Snapp, N.; Akimov, A. V.; Hongkun, P.; et al. Near-Field Electrical Detection of Optical Plasmons and Single-Plasmon Sources. *Nat. Phys.* **2009**, *5* (7), 475–479.

- (15) Moskowitz, J.; Geddes, C. Plasmonic Electricity: Fluorophore-Induced Plasmonic Current. *J. Phys. Chem. C* **2019**, *123* (45), 27770–27777.

- (16) Moskowitz, J.; Sindi, R.; Geddes, C. Plasmonic Electricity II: The Effect of Particle Size, Solvent Permittivity, Applied Voltage, and Temperature on Fluorophore-Induced Plasmonic Current. *J. Phys. Chem. C* **2020**, *124*, 5780–5788.

- (17) Knoblauch, R.; Moskowitz, J.; Hawkins, E.; Geddes, C. D. Fluorophore-Induced Plasmonic Current: Generation-Based Detection of Singlet Oxygen. *ACS Sensors*. **2020**, *5* (4), 1223–1229.

- (18) Novotny, L.; van Hulst, N. Antennas For Light. *Nat. Photonics* **2011**, *5* (2), 83–90.

- (19) Moore, R. G. C.; Evans, S. D.; Shen, T.; Hodson, C. E. C. Room-Temperature Single-Electron Tunnelling in Surfactant Stabilised Iron Oxide Nanoparticles. *Phys. E* **2001**, *9* (2), 253–261.

- (20) Schmid, G. D. *Nanoparticles: From Theory to Application*; Wiley-VC: Weinheim, 2004.

- (21) Markovich, G.; Collier, C. P.; Heath, J. R. Reversible Metal-Insulator Transition in Ordered Metal Nanocrystal Monolayers Observed by Impedance Spectroscopy. *Phys. Rev. Lett.* **1998**, *80* (17), 3807–3810.

- (22) Kano, S.; Tanaka, D.; Sakamoto, M.; Teranishi, T.; Majima, Y. Control of Charging Energy in Chemically Assembled Nanoparticle Single-Electron Transistors. *Nanotechnology* **2015**, *26* (4), 045702–045702.

- (23) Negishi, R.; Hasegawa, T.; Tanaka, H.; Terabe, K.; Ozawa, H.; Ogawa, T.; Aono, M. Size-Dependent Single Electron Tunneling Effect In Au Nanoparticles. *Surf. Sci.* **2007**, *601*, 3907–3911.

(24) Garcia-Morales, V.; Mafe, S. Monolayer-Protected Metallic Nanoparticles: Limitations of The Concentric Sphere Capacitor Model. *J. Phys. Chem. C* **2007**, *111* (20), 7242–7250.

(25) Weaver, M. J.; Gao, X. Molecular Capacitance: Sequential Electron-Transfer Energetics For Solution-Phase Metallic Clusters In Relation To Gas-Phase Clusters And Analogous Interfaces. *J. Phys. Chem.* **1993**, *97* (2), 332–332.

(26) Li, D.; Li, J. Preparation, Characterization And Quantized Capacitance Of 3-Mercapto-1,2-Propanediol Monolayer Protected Gold Nanoparticles. *Chem. Phys. Lett.* **2003**, *372* (5), 668–673.

(27) Wolfe, R. L.; Murray, R. W. Analytical Evidence For The Monolayer-Protected Cluster Au₂₂₅[(S(CH₂)₅CH₃)]₇₅. *Anal. Chem.* **2006**, *78* (4), 1167–1173.

(28) Geddes, C. D.; Cao, H.; Lakowicz, J. R. Enhanced Photostability of ICG in Close Proximity to Gold Colloids. *Spectrochim. Acta, Part A* **2003**, *59*, 2611–2617.

(29) Lakowicz, J. R.; Gryczynski, I.; Malicka, J.; Gryczynski, Z.; Geddes, C. D. Enhanced and localized multiphoton excited fluorescence near metallic silver islands: metallic islands can increase probe photostability. *J. Fluoresc.* **2002**, *12*, 299–302.

(30) Zhang, Y.; Aslan, K.; Geddes, C. D. Voltage-Gated Metal-Enhanced Fluorescence. *J. Fluoresc.* **2009**, *19* (2), 363–367.

(31) Dragan, A. I.; Zhang, Y.; Geddes, C. D. Voltage-Gated Metal-Enhanced Fluorescence II: Effects of Fluorophore Concentration on the Magnitude of the Gated Current. *J. Fluoresc.* **2009**, *19* (2), 369–374.